momentum-transfer distribution or of 3-3 isobar production.[23]

4. If the A_1 is a resonance, then our most likely assignments for its spin parity are $J^P=1^+$ (s wave) or 2^-.

5. The most likely spin parity assignments for the A_2

---

[23] Barnes *et al.* (Ref. 22) state that they have no peak in the A_1 region when the isobar events are removed. Their data do show an excess of events in the A_1 region after the subtraction, but this excess is in the form of a broad shoulder rather than a peak. The number of events in our experiment is too small to tell the difference between a peak and a shoulder, but we can tell that there is an excess of events in the A_1 region after subtracting isobar events.

are $J^P=2^-$, 1^-, or 1^+ in our highly model-dependent calculation.

ACKNOWLEDGMENTS

Polarization Parameter in p-p Scattering from 328 to 736 MeV*

F. Betz,† J. Arens, O. Chamberlain, H. Dost,‡ P. Grannis, M. Hansroul, L. Holloway, C. Schultz,§ and G. Shapiro

Lawrence Radiation Laboratory, University of California, Berkeley, California

(Received 17 March 1966)

The polarization parameter in elastic proton-proton scattering has been measured using an unpolarized proton beam and a polarized proton target. Measurements were taken at laboratory kinetic energies of 328, 614, 679, and 736 MeV in the angular regions from 33 to 110 degrees center-of-mass. The results indicate that the maximum polarization at a given energy increases in the region from 328 to 679 MeV. At 328 MeV the results are in good agreement with those of a previous experiment at 315 MeV performed by the double-scattering technique.

I. INTRODUCTION

ALTHOUGH the phenomenological description of the proton-proton interaction has been in a fairly satisfactory state for several years up to kinetic energy 300 MeV,[1] extension of this knowledge to higher energies has been slow, owing in part to the relative scarceness of experimental data, and in part to the rapidly increasing number of parameters required.[2] From the work done up to 300 MeV, as well as that on the pion-nucleon interaction,[3] it appears that a promising road to a satisfactory description of the nucleon-nucleon interaction lies in an energy-dependent phase-shift analysis. For this reason we have measured the polarization in elastic p-p scattering at several energies between 300 and 740 MeV. The availability of a polarized proton

target enabled us to take data at a greatly increased rate compared to the formerly used double-scattering technique, as well as at many angles simultaneously, and also enabled us to avoid some of the sources of systematic errors common in double-scattering experiments, such as spurious asymmetries due to counter misalignment and uncertainties in the angular and energy dependence of the analyzing power.

Because of the spin-state multiplicity of the nucleon-nucleon system, a large number of independent experiments must be performed at each energy if the phenomenological analysis is to have any hope of success. These include, in addition to cross-section and polarization measurements, "triple-scattering" and spin-correlation experiments as well as investigations of the inelastic processes. Some of these have been performed at various laboratories, and we have recently completed a measurement of C_{NN} as a function of angle at 680 MeV, using a polarized beam and polarized target.[4] Still, a number of other types of experiments will be needed before a phase-shift analysis can be completed.

The formal description of nucleon-nucleon scattering has been carried out by a large number of authors in

---

[1] M. H. MacGregor, M. J. Moravcsik, and H. P. Strapp, Ann. Rev. Nucl. Sci. **10**, 291 (1960).
[2] See, however, R. Ya. Zue'karnerv and I. N. Silin, Phys. Letters **3**, 265 (1963); N. Hoshizaki and S. Machida, Research Institute of Fundamental Physics Report No. RIFP-30, Kyoto University, 1963 (unpublished).
[3] L. D. Roper and R. M. Wright, Phys. Rev. **138**, B921 (1965).

[4] H. E. Dost, J. F. Arens, F. W. Betz, O. Chamberlain, M. J. Hansroul, L. E. Holloway, C. H. Schultz, and G. Shapiro, Bull. Am. Phys. Soc. **9**, 724 (1964).

various degrees of completeness and complexity.[5] We present only those ideas directly pertinent to this experiment. In a proton-proton scattering experiment in which one of the initial-state protons is polarized, the angular distribution of scattered protons is given by

$$I(\theta,\varphi) = I_0(\theta,\varphi)[1 + \mathbf{P}_i \cdot \mathbf{P}'(\theta)], \tag{I.1}$$

where $I_0(\theta,\varphi)$ is the angular distribution if both incident protons are unpolarized, $\mathbf{P}_i$ is the polarization of the polarized initial-state proton, and $\mathbf{P}'(\theta)$ is the analyzing power in p-p scattering, defined as

$$I_0\mathbf{P}'(\theta) = \tfrac{1}{4}\,\mathrm{Tr}M\boldsymbol{\sigma}M^\dagger, \tag{I.2}$$

and the direction of $\mathbf{P}'(\theta)$ may be shown to be parallel or antiparallel to the normal to the scattering plane if one assumes parity conservation. In Eq. (I.2), M is the scattering matrix, and by $\boldsymbol{\sigma}$ we mean the direct product of the Pauli spin matrix for the polarized initial-state proton and the 2×2 unit matrix for the unpolarized proton. $P'(\theta)$ is the azimuthal asymmetry resulting if the polarized incident protons are 100% polarized, where asymmetry ϵ is

$$\epsilon = \frac{I(\theta,\varphi=0) - I(\theta,\varphi=\pi)}{I(\theta,\varphi=0) + I(\theta,\varphi=\pi)}$$

and $\varphi=0$ indicates that P_i and P' are parallel, $\varphi=\pi$ indicates they are antiparallel. For the purpose of measuring $P'(\theta)$, it is immaterial which incident proton—beam or target—is polarized. Since the discovery of polarization effects in high-energy scattering, such measurements have been made by forming a polarized beam through scattering. This experiment[6] and the one reported in the following paper[7] were the first measurements of $P'(\theta)$ which used a polarized target.[8]

Under the assumption of parity and time-reversal invariance of M, $\mathbf{P}'(\theta)$ is equal to the polarization $\mathbf{P}(\theta)$, defined as

$$\mathbf{P}(\theta) = \tfrac{1}{4}\,\mathrm{Tr}MM^\dagger\boldsymbol{\sigma}.$$

$\mathbf{P}(\theta)$ is the polarization that results from scattering unpolarized incident particles at the given angle and energy. In fact, in the literature the two quantities $\mathbf{P}(\theta)$ and $\mathbf{P}'(\theta)$ have usually been used interchangeably, and we follow this practice by referring to our result as

the "polarization parameter." This polarization parameter as defined by Eq. (I.1) is also correct relativistically, as pointed out in the following paper.

II. EXPERIMENTAL ARRANGEMENT

A. Beam

The Berkeley 184-in. synchrocyclotron accelerated protons to a fixed energy. Various thicknesses of absorber were used to degrade this maximum energy to lower energies. The manner in which the proton beam was formed makes it unlikely to have had any significant degree of polarization. In addition, the symmetry of the arrangement prohibited introducing any polarization that had a component perpendicular to the plane of the scattering. Figure 1 shows a diagram of the beam system. The plane of the scattering was vertical.

The energies of the beams were measured by a range telescope; the beam energies used were 736 ± 5 MeV, 679 ± 7 MeV, 614 ± 5 MeV, and 328 ± 6 MeV. At energies 736, 679, and 328 MeV, the beam spots at the target were from 1.5 to 2 times the area of the target. At 614 MeV, the beam spot was approximately the size of the target.

In order to keep the rate of accidental events counted by the detection system at a small fraction of the total rate, the beam intensity was held below 10^8 protons/sec during all data-taking. Variations in beam intensity of a factor of 2 did not change either the rate of hydrogen events or the background rate. The beam was used in the "stretched" mode, providing a spill of 12-msec duration with a repetition rate of 64 per sec.

B. Target

The polarized target used in the experiment has been described elsewhere in detail.[9,10] Only a brief summary is given here.

The target itself consists of four single crystals of $La_2Mg_3(NO_3)_{12}\cdot24H_2O$. A small fraction of the La ions have been replaced with the paramagnetic ions of Nd^{142}, and the hydrogen nuclei in the waters of hydration are polarized by the technique of dynamic nuclear orientation.[11] The hydrogen nuclei provided a polarized proton target with an equivalent thickness of $0.15\mathrm{g/cm^2}$.

The crystals are cooled in a liquid-helium bath whose temperature has been lowered to about $1.2°\mathrm{K}$ by decreasing the vapor pressure of the helium with a mechanical pump. An external magnetic field of 18.75 kG applied to the crystals splits the two spin states of the spin-$\tfrac{1}{2}$ protons. The polarization of the target is

[5] L. Wolfenstein, Ann. Rev. Nucl. Sci. **6**, 43 (1956); Michael J. Moravcsik, *The Two-Nucleon Interaction* (Clarendon Press, Oxford, England, 1963) and references cited therein.

[6] Preliminary results of this experiment were presented in *Proceedings of the International Conference on High Energy Physics, Dubna, 1964* (Atomizdat, Moscow, 1965).

[7] P. Grannis *et al.*, following paper, Phys. Rev. **148**, 1297 (1966).

[8] An earlier p-p experiment, at low energy, using a polarized target, was done at Saclay: A. Abragam, M. Borghini, P. Catillon, J. Coustham, P. Roubeau, and J. Thirion, Phys. Letters **2**, 310 (1962). An earlier high-energy π-p experiment, done with our target, is: O. Chamberlain, C. D. Jeffries, C. H. Schultz, G. Shapiro, and L. Van Rossum, *ibid.* **7**, 293 (1963).

[9] C. H. Schultz, Ph.D. thesis, University of California Radiation Laboratory Report No. UCRL 11149 (unpublished).

[10] G. Shapiro, Progr. Nucl. Tech. Instr. **1**, 173 (1964).

[11] C. D. Jeffries, *Dynamic Nuclear Orientation* (Interscience Publishers, Inc., New York, 1963).
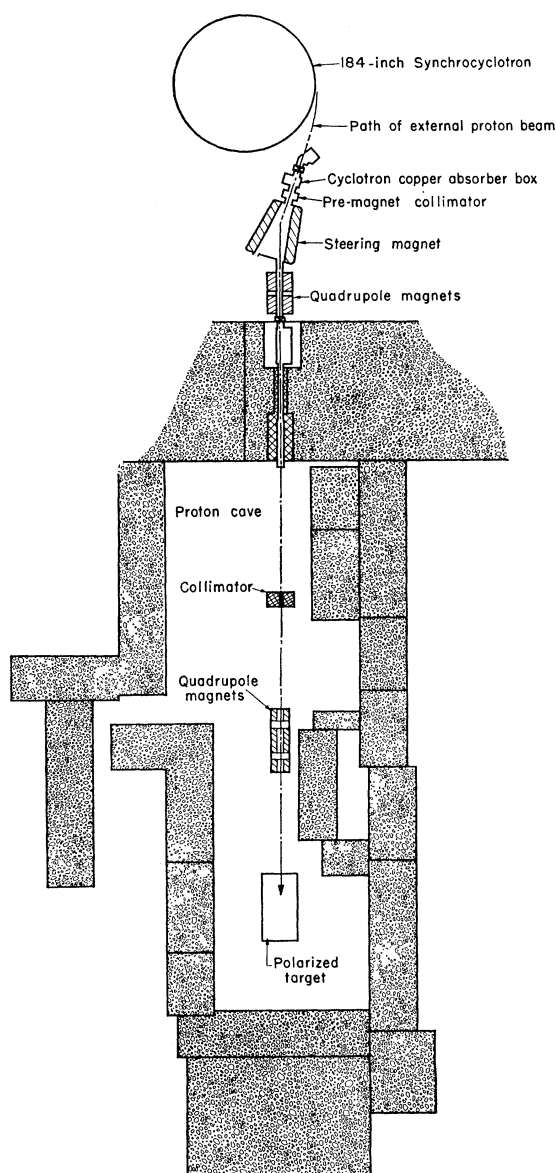
Fig. 1. Proton-beam-transport system.

defined as the fractional difference in the population densities of these spin states

$$P_T = \frac{N(+\tfrac{1}{2}) - N(-\tfrac{1}{2})}{N(+\tfrac{1}{2}) + N(-\tfrac{1}{2})}. \qquad (II.1)$$

At this temperature and field the Boltzman distributions in the two energy states provide a "natural" polarization of 0.16%. To attain higher polarizations of either sign, the crystals are irradiated with microwaves of frequencies near the electron resonance (71 kMc/sec for 18.75 kG.) The paramagnetic Nd[142] ions at this temperature behave like spin-$\tfrac{1}{2}$ electrons with an effective g factor of 2.70. These ions can be thought of as

unpaired electrons whose spins couple with the spins of neighboring protons of the hydrogen nuclei.

When the microwave frequency is appropriate for saturating one of the forbidden transitions, corresponding to simultaneous proton and electron spin flips, large proton polarizations are induced. It is important that the relaxation time for the "electron" spin flip be much less than the relaxation time for the proton spin flip. For the present target the relaxation time for the electron spin flip is of the order of milliseconds, whereas that of the proton flip is about 15 min. Thus each neodymium ion can successively flip many neighboring proton spins. Further propagation of the proton polarization outward from the neighborhood of the neodymium center depends on proton-proton spin interactions, which cause mutual flips of neighboring protons. From the definition of the polarization and by applying the Boltzmann factor in the usual way, one obtains the "natural" polarization of the protons—in thermal equilibrium with the liquid-helium bath at temperature T and in the external magnetic field H_0—to be

$$P_0 = \tanh(\mu_p H_0/2kT). \qquad (II.2)$$

When one of the forbidden transitions is saturated, the proton polarization should approach

$$P_T = \tanh(\mu_e H_0/2kT). \qquad (II.3)$$

At the field and temperature used, this is about 88%. For various reasons,[9] the theoretical value is not reached. During the experiment, the average target polarization was 40%.[12]

An extremely important feature of the polarized target is that high polarizations can be obtained along either of two opposite directions—parallel or antiparallel to the external magnetic field—without reversing the field, by the proper choice of forbidden transition.[9,10] The direction of polarization can be reversed in about 15 min by changing the microwave frequency by 0.2%.

In the scattering experiment the elements in the target, other than hydrogen, generated background events. The detected background events were primarily of two kinds: quasielastic scatterings of incident beam protons with bound protons in the nuclei of the non-hydrogen elements, and accidental coincidences between scattered protons from different scatterings occurring within the resolution time of the coincidence circuit. To evaluate the shape of the background, we constructed a dummy target to simulate the crystal target in kinds of atoms and in their respective proportions by weight. At each measured counter position and energy, runs were also made with the dummy target. Attempts were made to keep all other conditions of the experimental setup identical between the set of dummy target runs and the crystal target runs.

---

[12] In our subsequent experiments, typical target polarizations have been raised to well over 50%, reaching up to 65%.
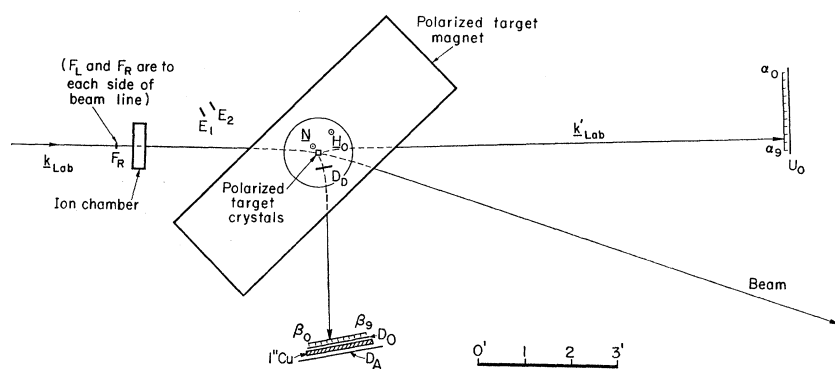
Fig. 2. Arrangement of the scintillation counters. Typical dimensions for the α and β counters were $1.5 \times 1.5 \times 0.5$ in. The direction of the normal to the scattering plane N and of the polarized-target external magnetic field H_0 are indicated.

C. Experimental Arrangement

An upper and a lower array of 10 scintillation counters each were used to detect the elastically scattered protons. A count was stored in a coded bin of a 100-channel analyzer for each event detected, as an element of a 10×10 matrix. Figure 2 depicts the counter arrangement. The dimensions of the counters and their distances from the target were chosen to maximize the ratio of the elastic p-p scatterings to the background, consistent with the desired angular resolution and counting rate.

Since quasielastic scatterings of protons in the beam with protons in the nuclei of the nonhydrogen elements of the target were prime contributors to the background, advantage was taken of the fact that these protons in the nuclei have an average Fermi momentum of 200 (MeV/c). The orientation of this momentum is random, and its effect is to smear the trajectories of the scattering particles through an angle $\theta \approx 200 \ (\text{MeV}/c)/p_j \ (\text{MeV}/c)$ centered about the trajectories an elastic scattering would have had for the same center-of-mass-angle scattering (here p_j represents the lab momentum of either scattered particle).

Counters D_A, D_0, and D_D provided a telescope looking at the target. Their coincidence was used as a monitor to normalize the length of each run. The ion chamber and a two-counter telescope, $E_1 E_2$ (that looked at the ion chamber), were additional monitors independent of the normalizing monitor and the crystal target.

The center-of-mass scattering angles of events detected by the counter matrix were determined by kinematically tracing trajectories from the center of the target to the counter arrays in the laboratory frame. We estimate that the calculated angles are correct to $\pm 1°$ center-of-mass.

An experimental measurement of $P(\theta)$, at a given energy and with a given setting of the counters, consisted of storing elastic p-p events under conditions in which only the sign and magnitude of the target polarization were allowed to change. Events were stored for a given number of monitor counts with the spins of the target protons aligned parallel to the normal to the plane of scattering and then for an equal number of monitor counts with the spins antiparallel. The target polarization was reversed about once an hour.

III. MEASUREMENT OF THE TARGET POLARIZATION

The polarization of the free protons in the target was measured by monitoring their nuclear magnetic resonance signal. The crystals were positioned in the center of an rf pickup coil that consisted of two rectangular "figure-eight" loops. Figure 3 shows a sketch of the crystals and NMR pickup coil. Two crystals were fastened to each side of the aluminum septum used to guide the rf flux lines into a more uniform rf magnetic field configuration in the region occupied by the crystals. The leads from the coil were connected in parallel with a variable capacitance, forming an effective parallel capacitance-inductance circuit. Figure 4 is a schematic diagram of the detection system. An rf signal generator drove the circuit at resonance. This generator fed the tuned circuit through such a large capacitive reactance X_s that it could be considered
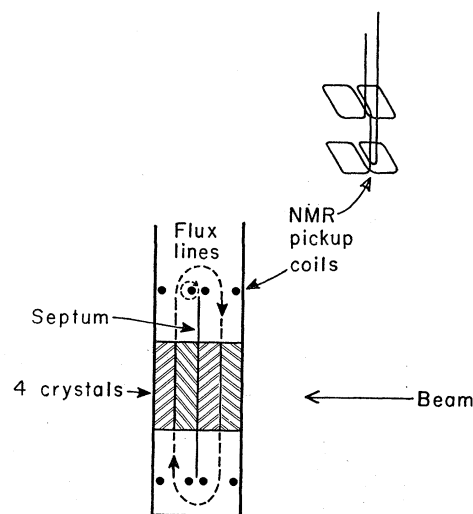

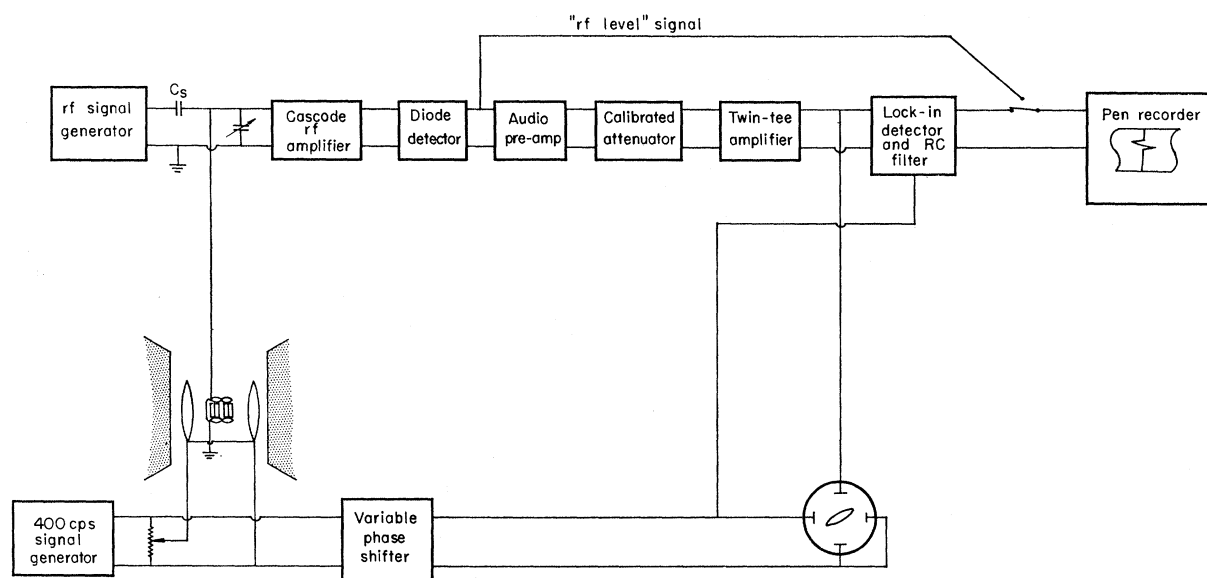Fig. 3. Sketch of the polarized-target crystals and the NMR pickup coils.

Fig. 4. Schematic diagram of the NMR detection system.

as a constant current source. When the frequency of the rf generator passed through the proton resonance value ν_p appropriate to external magnetic field H_0, the proton spin system absorbed or emitted energy to the rf field (depending upon whether the protons they were aligned predominantly parallel or antiparallel to the field). This appeared in the resonance circuit as a change in the impedance of the circuit. Since the rf generator effectively generated a constant current, this change in impedance was detected by measuring the linearly related voltage change of the circuit. To facilitate the observation of this signal, the external magnetic field was perturbed with a small alternating 400-cps component. This was achieved by a pair of coils (of approximate Helmholtz geometry) placed against the pole faces of the target magnet and fed by an alternating current of 400 cps. The magnitude of this current was restricted so that the perturbation would not be large enough to disturb the stability of the polarization method. This perturbation of the field manifests itself in the detection system as a 400-cps amplitude modulation on the rf voltage. The rf voltage across the resonance circuit was amplified and then, by means of a diode, rectified. The diode voltage gave a 400-cps signal whose amplitude was proportional to the slope of the proton-resonance-absorption curve. This signal was amplified and converted by a lock-in phase-sensitive detector to a proportional dc signal. This signal, representing the derivative of the NMR line, is called the differential signal. It was recorded on a chart recorder and simultaneously digitized and recorded on paper tape. Concurrently the dc voltage level of the rf rectifying diode was digitized and recorded.

A complex rf susceptibility $\chi = \chi' - i\chi''$ can be defined for the crystals. The complex susceptibility χ is pro-

portional to the polarization P_T. Although the rf susceptibility of the crystal cannot be derived from a single Lorentz shape, it can be thought of as a linear sum of the 48 single-proton resonances in the crystal molecule. A line-shape factor $g(\omega - \gamma H)$ can be defined for the system such that

$$\chi''(\omega, H) \propto P_T g(\omega - \gamma H); \qquad \text{(III.1)}$$

that is, g is proportional to the absorption line shape. Here ω is the rf angular frequency, γ is the proton gryomagnetic ratio, and H is the external magnetic field, including the 400-cps perturbing component.

The integral of $g(\omega - \gamma H)$ over all frequencies is a real constant, and g is usually normalized to make it unity. The shape of g, however, while remaining fairly constant up to polarizations of 10%, changes quite drastically for higher polarizations due to the changing polarization of the nearest-neighbor protons, which affects the local field (cf. Figs. 14–16 of Ref. 9). Because of this effect, the amplitude of the proton magnetic resonance cannot be used as a measure of the polarization; however, the area under the absorption curve *is* a good measure, as will be shown.

The complex impedance Z of the tuned circuit can be written as

$$\frac{1}{Z} = \frac{1}{Z_L} + \frac{1}{Z_C}, \qquad \text{(III.2)}$$

where $Z_C = 1/i\omega C$, and C is the value of the parallel capacitance. The impedance Z_L is the sum of resistive and inductive impedance of the circuit.

$$Z_L = R + i\omega L(1 + 4\pi\eta\chi), \qquad \text{(III.3)}$$

where L is the inductance of the coil in the absence of

resonance absorbtion and η is the fraction of the volume of the coil occupied by the crystals.

The quantities detected were V and $\partial V/\partial H$ (where V is the peak voltage across the circuit), which, assuming a constant current source are proportional to $|Z|$ and $\partial|Z|/\partial H$, respectively. Since the circuit has a large, nearly real impedance near resonance, and since in practice $\omega L\chi \ll R \ll \omega L$, the expression for $|Z|$ reduces to

$$|Z| = (\omega L)^2/(R+4\pi\eta\omega L\chi'').\qquad\text{(III.4)}$$

Hence[13]

$$\frac{\partial|Z|}{\partial H}=\frac{-4\pi\eta(\omega L)^3}{(R+4\pi\eta\omega L\chi'')}\frac{\partial\chi''}{\partial H},\qquad\text{(III.5)}$$

and

$$\frac{1}{V^2}\frac{\partial V}{\partial H}\propto\frac{1}{|Z|^2}\frac{\partial|Z|}{\partial H}=-\frac{4\pi\eta}{\omega L}\frac{\partial\chi''}{\partial H}$$

$$\propto-P_T\frac{\partial g(\omega-\gamma H)}{\partial H}\propto P_T\frac{\partial g}{\partial\omega},\quad\text{(III.6)}$$

using the definition (III.1). Finally

$$\int_0^\infty d\omega\int_0^\omega d\omega'\frac{1}{V(\omega')^2}\frac{\partial V(\omega')}{\partial H}$$

$$\propto P_T\int_0^\infty d\omega\int_0^\omega d\omega'\frac{\partial g(\omega'-\gamma H)}{\partial\omega'}=P_T,\quad\text{(III.7)}$$

because of the normalization of g. Thus a double integration, with respect to frequency, of the detected differential signal divided by the square of the dc voltage of the rectifying diode gives a quantity proportional to the polarization of the target. The double integrations of Eq. (III.7) were done numerically on an IBM-7094 computer.

The procedure for calibration of the target polarization measurement consisted of recording the NMR proton signal when the crystals were in thermal equilibrium with the liquid helium bath and no microwaves were present to stimulate the "forbidden transitions." This signal was called the thermal equilibrium (TE) signal. While such a TE signal was being recorded, the vapor pressure of the liquid helium was measured with an oil manometer and the central rf frequency at which the resonance occurred was noted. The vapor pressure is effectively a measure of the temperature of the system, and the central-resonance frequency a measure of the strength of the external field. The absolute magnitude of the target

---

[13] To be exact, one should carry out the differentiation *before* making the approximations. The calculation is carried out fully in Ref. 9, using numbers appropriate to an earlier version of our detection system. With numbers appropriate to this experiment, Eq. (III.5) is good to about 1%.

polarization is computed under these conditions from Eq. (II.2).

The double integration (III.7) for the TE signals was then compared with the enhanced signals to give the absolute polarization.

IV. ANALYSIS OF DATA

In the center-of-mass system, a counter of the upper array defined a solid angle $\Delta\Omega$ at an angle θ. The number of counts in this counter that were accumulated during an ith run can be written as

$$N_i=m_iI_0[1+P_{Ti}P(\theta)]+m_iB,\qquad\text{(IV.1)}$$

where

$m_i=$ monitor counts $[m_i\propto$ number of incident protons$\times$solid angle of counter (as long as the counter positions are held fixed)$]$;

$I_0=$ unpolarized differential cross section for elastic p-p scattering in c.m. system;

$P_{Ti}=$ polarization of target during ith run, taken to be positive when it was parallel to $\mathbf{k}\times\mathbf{k}'$, where $\mathbf{k}$ and $\mathbf{k}'$ are the incident and outgoing proton momenta;

$P(\theta)=$ polarization parameter in p-p scattering;

$B=$ background contribution per unit monitor.

In order to subtract the background, runs taken with the dummy target were normalized to the total of the runs taken with the polarized target. To evaluate the polarization parameter $P(\theta)$ from the data, the hydrogen counts versus target polarization were fitted to a straight line by the method of least squares.

The principal sources of error are:

(a) Statistics of the counts in the hydrogen-peak region for each upper array counter.

(b) Statistics of the counts of the dummy target in the region where the hydrogen peaks would have been.

(c) Statistics in the flat regions of the matrix that are used to normalize the dummy target.

(d) Statistics in the monitor coincidences used to normalize the runs.

(e) The estimation of the average polarization of the target during a run. The error in P_{Ti}, is determined from the scatter in a plot of calculated polarizations versus peak-to-peak recorded signals of the NMR proton resonance of the target, and ranged from 4.5 to 5.5%.

(f) In addition to the above sources of error a systematic error arose from measurements of (a) the area of the TE proton resonance signal and (b) the temperature of the liquid helium bath when the signal was recorded. The accuracy with which the oil manometer indicated the vapor pressure of the liquid helium contributed an uncertainty of 3% in the value of the absolute polarization of the average TE signal. The average area of the TE signals was estimated to be good to $\pm5\%$. Combining these errors in quadrature gives
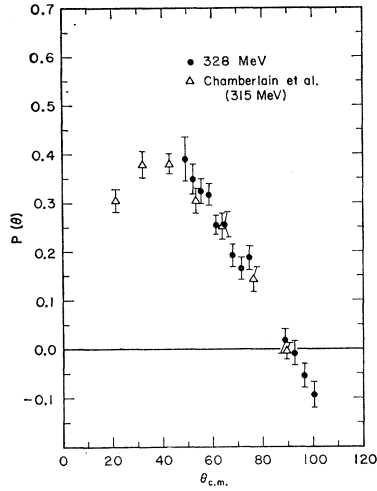
FIG. 5. The measured values of $P(\theta)$ in p-p scattering at 328 MeV. The errors shown do not include systematic errors (see Table I). Shown for comparison are the data of Chamberlain, Segrè, Tripp, Wiegand, and Ypsilantis (Ref. 15).

systematic error of 5.83% to be added, in quadrature, to the other sources of error.

If the polarization is not uniform in the target, a systematic error can be introduced. Early in the experiment, after some data had been taken, a small beam of approximately $\frac{1}{4}$-in. diam. was focused on various parts of the target and the asymmetry in counting rate for each part was measured. In this manner a contour diagram of polarization in the target was obtained. A correction[14] was made to the data at 614 MeV, for effects of nonuniform target polarization. At other energies conditions were such that no correction was necessary.

V. RESULTS

The measured values of the polarization parameter $P(\theta)$ in elastic proton-proton scattering are presented in Tables I–IV and graphed in the Figs. 5–8. Given

TABLE I. Polarization parameter $P(\theta)$ in elastic p-p scattering for incident kinetic energy of 328 ± 6 MeV.[a]

$-t[(\mathrm{BeV}/c)^2]$ ±0.006	$\theta_{\mathrm{c.m.}}$ $\pm1°$	$P(\theta)$	$\Delta P(\theta)$
0.107	49.1	0.389	0.045
0.119	52.2	0.349	0.031
0.133	55.3	0.324	0.025
0.147	58.4	0.317	0.022
0.162	61.6	0.255	0.020
0.177	64.8	0.256	0.027
0.193	68.1	0.191	0.024
0.210	71.4	0.165	0.023
0.227	74.7	0.187	0.023
0.283	85.3	0.163	0.035
0.302	88.9	0.016	0.027
0.322	92.6	−0.008	0.025
0.343	96.5	−0.054	0.024
0.365	100.6	−0.094	0.027

[a] A systematic error of $(_{-5.8}{}^{+6.5}\%) \times P$ must be added in quadrature to the above errors $\Delta P(\theta)$.

[14] F. W. Betz, Ph.D. thesis, University of California Radiation Laboratory Report No. UCRL 11565 (unpublished).

TABLE II. Polarization parameter $P(\theta)$ in elastic p-p scattering for incident lab kinetic energy of 614 ± 5 MeV.[a]

$-t[(\mathrm{BeV}/c)^2]$ ±0.015	$\theta_{\mathrm{c.m.}}$ $\pm2°$	$P(\theta)$	$\Delta P(\theta)$
0.271	58.0	0.505	0.019
0.313	62.8	0.492	0.019
0.344	66.2	0.413	0.020
0.356	67.5	0.463	0.019
0.397	71.9	0.325	0.018
0.401	72.3	0.357	0.019
0.453	77.6	0.238	0.016
0.511	83.5	0.091	0.015

[a] A systematic error of $(\pm19\%) \times P$ must be added in quadrature to the above errors $\Delta P(\theta)$.

TABLE III. Polarization parameter $P(\theta)$ in elastic p-p scattering for incident lab kinetic energy of 679 MeV.[a]

$-t[(\mathrm{BeV}/c)^2]$ ±0.01	$\theta_{\mathrm{c.m.}}$ $\pm1°$	$P(\theta)$	$\Delta P(\theta)$
0.141	38.8	0.578	0.028
0.163	41.9	0.578	0.019
0.186	45.0	0.583	0.017
0.212	48.1	0.596	0.017
0.238	51.2	0.570	0.013
0.266	54.3	0.529	0.013
0.294	57.4	0.484	0.018
0.324	60.5	0.430	0.017
0.354	63.7	0.399	0.018
0.386	66.7	0.363	0.019
0.427	70.8	0.293	0.030
0.458	73.7	0.274	0.027
0.490	76.7	0.247	0.031
0.522	79.6	0.151	0.036
0.555	82.6	0.073	0.044

[a] A systematic error of $(_{-5.8}{}^{+6.5}\%) \times P$ must be added in quadrature to the above errors $\Delta P(\theta)$.

TABLE IV. Polarization parameter $P(\theta)$ in elastic p-p scattering for incident lab kinetic energy 736 MeV.[a]

$-t[(\mathrm{BeV}/c)^2]$ ±0.006	$\theta_{\mathrm{c.m.}}$ $\pm1°$	$P(\theta)$	$\Delta P(\theta)$
0.108	32.5	0.579	0.049
0.129	35.6	0.579	0.028
0.152	38.8	0.553	0.017
0.177	42.0	0.560	0.014
0.203	45.1	0.559	0.015
0.231	48.3	0.528	0.011
0.260	51.4	0.520	0.011
0.291	54.6	0.497	0.013
0.322	57.7	0.498	0.013
0.354	60.9	0.473	0.014
0.404	65.5	0.419	0.018
0.437	68.4	0.365	0.017
0.470	71.4	0.342	0.018
0.504	74.3	0.304	0.018
0.538	77.2	0.231	0.018
0.573	80.2	0.180	0.018
0.609	83.2	0.144	0.023

[a] A systematic error of $(_{-5.8}{}^{+6.5}\%) \times P$ must be added in quadrature to the above errors $\Delta P(\theta)$.

with each of the values of the polarization parameter is the corresponding center-of-mass angle $\theta_{\mathrm{c.m.}}$ and the negative of the invariant square of the four-momentum transfer t. For elastic p-p scattering, t is related to
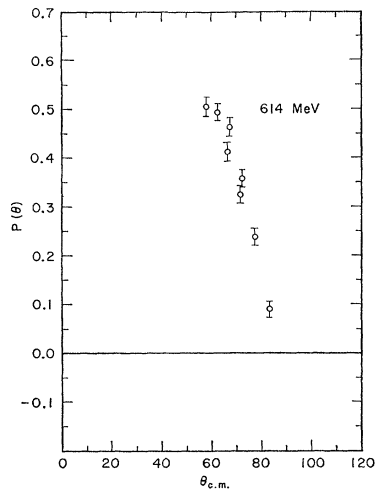
Fig. 6. The measured values of $P(\theta)$ in p-p scattering at 614 MeV. The errors shown do not include systematic errors (see Table II).
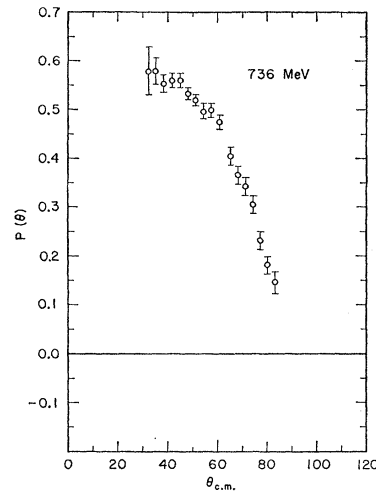
$\theta_{c.m.}$ by the expression $t = -2k^2(1 - \cos\theta_{c.m.})$, where k^2 is the square of the incident three-momentum in the center-of-mass system.

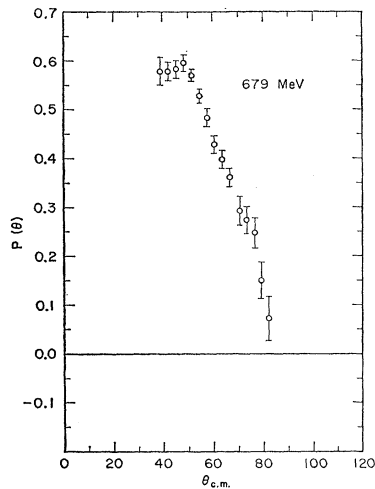Figure 5, which shows the plot of $P(\theta)$ at the energy of 328 MeV, contains also the values measured by

Fig. 7. The measured values of $P(\theta)$ in p-p scattering at 679 MeV. The errors shown do not include systematic errors (see Table III).

Fig. 8. The measured values of $P(\theta)$ in p-p scattering at 736 MeV. The errors shown do not include systematic errors (see Table IV).

Chamberlain *et al.*[15] in a double-scattering experiment. The agreement between the results of the two experiments might be regarded as evidence that our method of measuring the target polarization is satisfactory. Although we have not seen any reason to doubt this method, the agreement does represent the best check to date on our method of measuring target polarization.

VI. CONCLUSIONS

(1) The shape of the $P(\theta)$ curve is roughly the same at all the energies studied, showing a broad peak at about 40° c.m., and falling off at larger angles, to zero at 90° c.m.

(2) The maximum polarization as a function of energy has a peak at about 700 MeV, corresponding to a total energy in the center-of-mass system of 2210 MeV.

ACKNOWLEDGMENTS

We wish to thank J. Vale and the staff of the 184-in. cyclotron at Berkeley for their support.

[15] O. Chamberlain, E. Segrè, R. D. Tripp, C. Wiegand, and T. Ypsilantis, Phys. Rev. **105**, 288 (1957).